Journal of Atmospheric and Solar-Terrestrial Physics 78–79 (2012) 108–115

Contents lists available at ScienceDirect

Journal of Atmospheric and Solar-Terrestrial Physics

journal homepage: www.elsevier.com/locate/jastp

Variabilities of mesospheric tides during sudden stratospheric warming events of 2006 and 2009 and their relationship with ozone and water vapour

S. Sridharan [a,*], S. Sathishkumar [b], S. Gurubaran [b]

[a] National Atmospheric Research Laboratory, Gadanki 517112, India
[b] Equatorial Geophysical Research Laboratory, Indian Institute of Geomagnetism, Krishnapuram, Tirunelveli 627 011, India

ARTICLE INFO

Article history:
Received 30 October 2010
Received in revised form
22 February 2011
Accepted 15 March 2011
Available online 29 March 2011

Keywords:
Atmospheric tides
Ozone
Water vapour
Stratospheric warming

ABSTRACT

The present study demonstrates how the relationship between the high latitude northern hemispheric major sudden stratospheric warming (SSW) events of 2006 and 2009 and low-latitude mesospheric tidal variability in zonal winds observed by the MF radar at Tirunelveli (8.7°0N, 77.8°E) exists. It is found that the ozone mixing ratio increases at low latitudes during the SSW and it could probably be due to the SSW induced reversal of meridional circulation towards southward, which may aid the transport of ozone from high to low latitudes, but prevent the same from low to high latitudes. As semi-diurnal tide is produced due to solar insolation absorption of ozone and the increase in the ozone mixing ratio could be a reason for the increase in the semi-diurnal tidal amplitude. The variabilities of diurnal tide appear to be governed mostly by variation of specific humidity at 300 hPa over equator and intraseasonal variability dominates the variabilities in both the parameters.

1. Introduction

One of the most prominent phenomena observed in the winter stratosphere is the development of sudden stratospheric warming (SSW; see McIntyre (1982), for a tutorial review). These large disturbances are the consequence of the interactions between vertically propagating planetary waves and the zonal winds (Matsuno, 1971; Holton, 1976). These planetary waves produce a significant poleward and downward transport of lower-latitude ozone. Manney et al. (1994a) noted decrease of ozone in the Arctic lower stratosphere during February and early March 1993, when a major SSW event occurred and the decrease was attributed to chemical loss in the presence of nitrous oxide and methane, though dynamical effects were not altogether neglected. Understanding variabilities of ozone in particular during the SSW events is important to understand the variabilities of tides, as the forcing of the semi-diurnal tide, in particular, is mainly due to the absorption of ultraviolet radiation by ozone in the stratosphere and mesosphere. The stratospheric warming effects on tidal propagation at high latitudes have been reported in the past in a few studies (Bhattacharya et al., 2004; Hoffmann et al., 2007; Jacobi et al., 1999). Recently, Sridharan et al. (2009) noted enhancement in semi-diurnal tidal amplitude and suppression of diurnal tide in zonal winds at 88 km over Tirunelveli, a low-latitude site. As it is not clear how the low-latitude tidal variabilities are related to the occurrence of SSW events, Sridharan et al. (2009) suggested that the low-latitude mesospheric tidal variabilities during major SSW events could be ascribed to the non-linear interaction between tides and planetary waves, variability of ozone in the stratosphere and/or convective activity associated with latent heat release in the equatorial troposphere and subsequent to meridional circulation associated with the SSW events. Recently, Pedatella and Forbes (2010) demonstrated close relation between the planetary wave activity at high latitude northern hemisphere and non-migrating semi-diurnal tide in the low-latitude ionosphere. In the present paper, the ozone variabilities at high and low latitudes are reported during major warming events of 2006 and 2009 and their relationship with the variabilities of mesospheric tidal amplitudes at 90 km is presented.

2. Observations and data analysis

2.1. MF radar at Tirunelveli

The MF radar (1.98 MHz) at Tirunelveli (8.7°N, 77.8°E) has been giving nearly continuous wind information in the upper mesospheric region (78–98 km) since November 1992 (Rajaram and Gurubaran, 1998). The wind measurements, sampled for every 2 min, are averaged for each hour and used for further analysis. Though the winds are measured every 2 km, the data acceptance rate, based on several data rejection criteria (Briggs, 1984), is higher only above 84 km. Moreover, the wind measurements by the radar above 92 km appear to be contaminated by electric field

* Corresponding author. Tel.: +91 8585 272124; fax: +91 8585 272018.
E-mail addresses: SuSridharan@narl.gov.in, ssri_dhar@rediffmail.com (S. Sridharan).

1364-6826/$ - see front matter © 2011 Elsevier Ltd. All rights reserved.
doi:10.1016/j.jastp.2011.03.013

and the radar tends to measure electron drift motion rather than neutral winds at these heights (Gurubaran and Rajaram, 2000). Hence, for the present study, the tidal amplitudes are computed for zonal winds at 90 km using a least squares harmonic fit over a five-day composite window of hourly wind values, which is successively forwarded every day to obtain the daily variation. The five-day window is chosen so that it will average out all incoherent wind variations due mostly to gravity waves.

2.2. ERA-interim data

In this paper, we use a few ERA-Interim parameters, namely, zonal winds, temperature and specific humidity, available for the 37 pressure levels from the surface to 1 hPa at the ECMWF (European Center for Medium Range Weather Forecasting) website (http://www.ecmwf.int/research/era/do/get/index). These data were prepared by ECMWF using their variational data assimilation system. The ERA-interim data set consists of results from analysis conducted at six-hour intervals available for a 1.5° latitude–longitude grid.

2.3. SABER ozone and temperature observations

The present study also utilizes version 1.07 of processed level 2 ozone volume mixing ratio (VMR) and temperature data from the Sounding of the Atmosphere using Broadband Emission Radiometry (SABER) instrument on the Thermosphere, Ionosphere, Mesosphere, Energetics and Dynamics (TIMED) satellite available in the website http://saber.gats-inc.com/. The SABER uses CO_2 emission from two 15 μm channels for temperature profiles (Remsberg et al., 2008) and two independent techniques, 1.27 μm emission from molecular oxygen and the strong 9.6 μm emission from ozone itself, for determining ozone profiles in the mesosphere and lower thermosphere (Smith et al., 2009). The emission from ozone itself in the strong 9.6 μm band provides a method for observing ozone both day and night as the origin of this emission is thermal in nature. For the present study, ozone measurements at 9.6 μm are used. The ozone values are averaged for the latitudes 5°S–5°N, 5°N–15°N, 15°N–25°N and so on to represent, respectively, the latitudes 0°, 10°N, 20°N and so on. It may be noted that at mesospheric heights, ozone undergoes a significant diurnal variation. However, as daytime ozone data have many gaps, in order to maintain uniformity, zonal mean and night-time averaged ozone and also temperature are presented in this paper. There are gaps in the temperature and ozone data beyond 50°N poleward, at times, when the TIMED satellite yawed around and pointed SABER instrument towards southern hemisphere. The sampled local solar times of ozone and temperature by TIMED–SABER are given for both cases (2005–06 and 2008–09) in Fig. 1 for all latitudes. It may be noted that the sampled time is not same and there is a gradual change from one night to next night. It may affect the results only at upper mesospheric altitudes, where there is a change in the ozone mixing

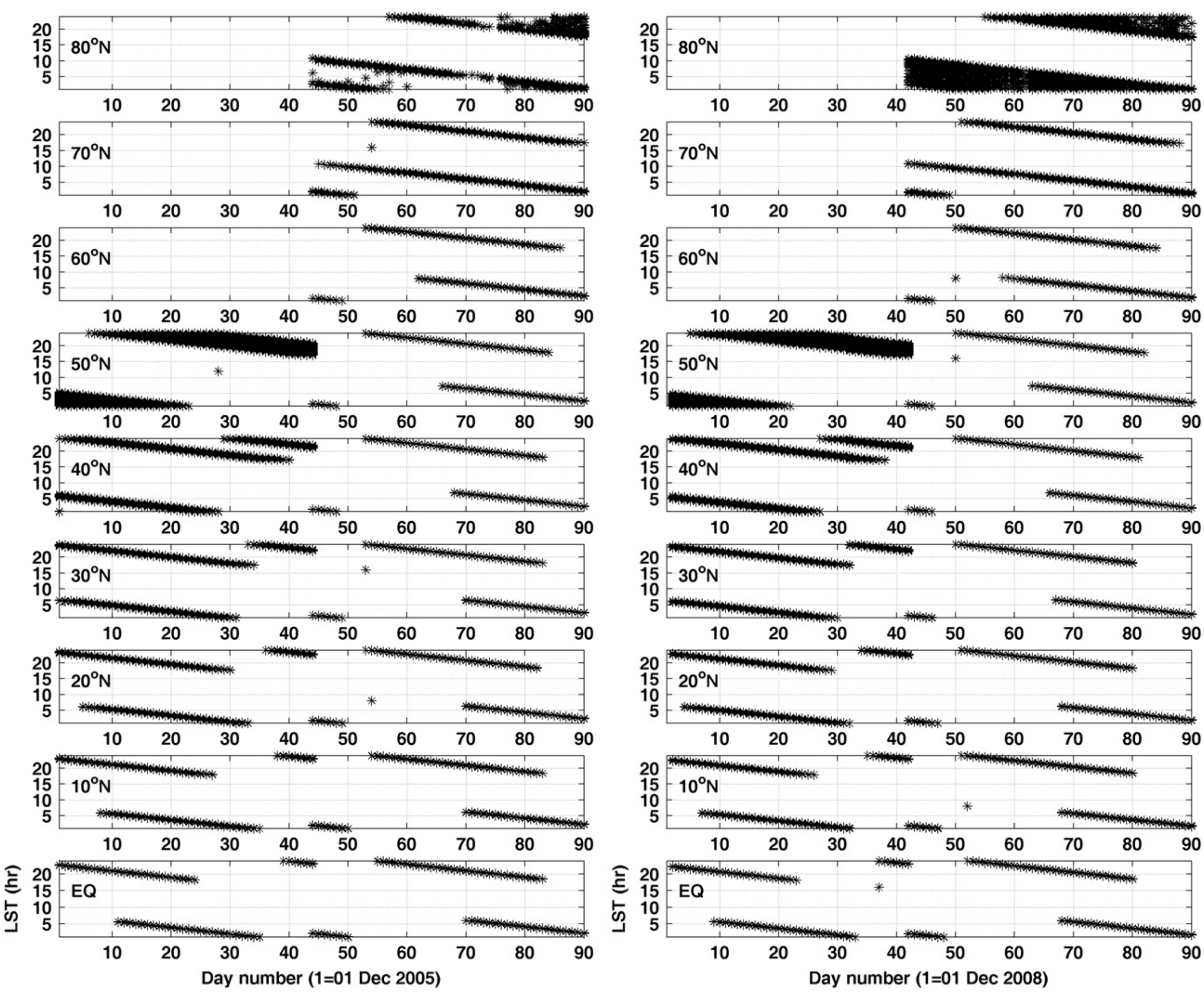

Fig. 1. Sampled local solar time of TIMED-SABER instrument during night-time for a time interval of 1–90 days starting from 01 December 2005 (left panels) and from 01 December 2008 (right panels).

ratio at sunrise and sunset hours (Rogers et al., 2009) and the local time variation may be interpreted as seasonal variation.

3. Results

Fig. 2a shows the daily variation of ERA-interim zonal mean temperature difference between the latitudes 90°N and 63°N and zonal mean zonal wind at 63°N at the pressure level of 10 hPa for 1–90 days starting from 01 December 2005. The temperature difference between the latitudes 90°N and 63°N shows that there are series of warming anomalies, which can be inferred from the positive temperature difference at 10 hPa during the day numbers 34–36, 40–49 and 52–68. The maximum temperature difference of 16, 20 and 32 K are observed on day numbers 35, 42 and 53 during the three warming cases, respectively. Though there are three successive warming events, only the third event is the major warming event, as it is accompanied by the reversal of zonal winds from eastward to westward. The zonal mean wind at 63°N starts decelerating after day number 25 (25 December 2005) itself, reverses its direction to westward on day number 52 (21 January 2006), attains maximum westward wind of 26 m/s on day number 57 (26 January 2006) and reverses again to eastward direction on day number 79 (17 February 2006). The 2006 SSW event is a remarkable event with an extended period of nearly one month of polar vortex disruption and zonal wind reversal observed in the lower and middle stratosphere and it is a polar vortex displacement event (Manney et al., 2008).

The daily variation of night-time ozone volume mixing ratio observed by TIMED-SABER at 50°N and at equator for the altitudes 20–100 km is shown in Fig. 2b and c, respectively. It may be noted that both day and night ozone can also have tidal signals that will vary daily due to the local time precession and therefore contribute to the day-to-day mesospheric variations. From the figure, we can infer that the high-latitude ozone VMR at 30–40 km and above 85 km responds well to the warming events. At 50°N, the VMR of ozone decreases from 6 ppm to less than 2 ppm above 85 km altitude during the warming events on day numbers 42 and 53. The low temperature around the day number 50 coincides with a slight increase in the ozone VMR. At equator, the VMR above 85 km altitude does not show any notable variation with the SSW events except that it shows marked rise in VMR coinciding with the onset of the major SSW and the increase in the VMR lasts until around day number 70 even after the end of the SSW event. At lower altitudes (30–40 km), the ozone VMR over equator responds well to the warming event. An increase in the VMR from 9 to 10 ppm can be observed around day number 30 coinciding with the increase of high-latitude stratospheric temperature and it remains at 10 ppm till the end of the observation period shown in the figure.

The latitudinal variations of temperature and ozone at 36 km are shown in Fig. 2d and e, respectively. During the SSW event, when the meridional temperature gradient reverses, with higher temperature (~245 K) at high latitudes and lower temperature at low latitude (230 K), the ozone VMR increases to 9.5 ppm during days 30–65 at latitudes 0–10°N and at 36 km, where semi-diurnal

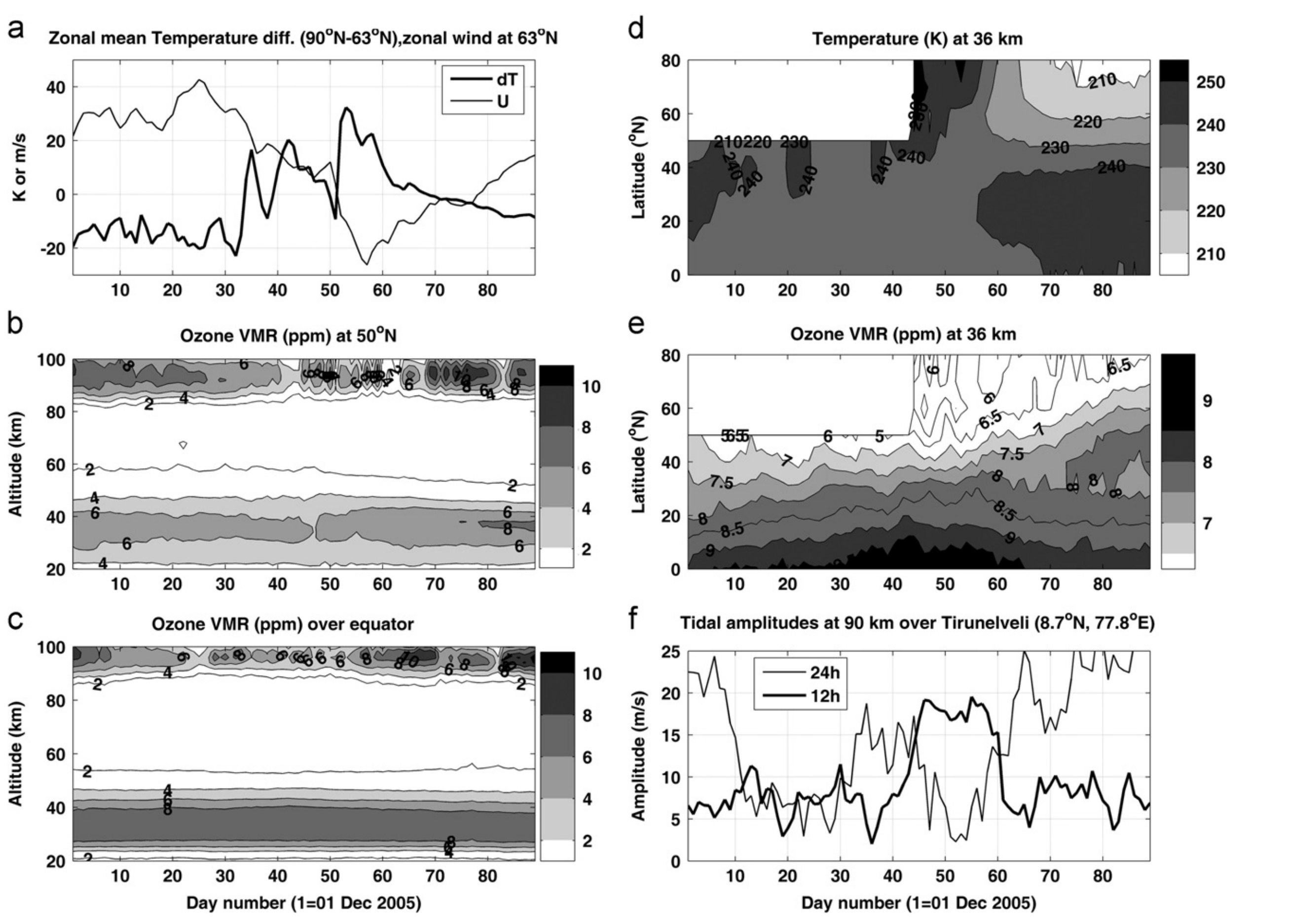

Fig. 2. (a) Daily variation of zonal mean temperature difference between the latitudes 90°N and 63°N and zonal mean zonal wind at 63°N and at 10 hPa. (b) and (c) Altitude variation of SABER ozone volume mixing ratio (VMR) at 50°N and at equator respectively, (d) latitude variation of temperature at 36 km, (e) latitude variation of ozone VMR at 36 km, (f) Diurnal (24 h) and semi-diurnal (12 h) tidal amplitudes in zonal winds at 90 km over Tirunelveli (8.7°N, 77.8°E) for a time interval of 1–90 days starting from 01 December 2005.

heating (2,2) is larger (Groves, 1982a). The large ozone value (10 ppm) over equator occurred during day numbers 40–45. The time variation of diurnal and semi-diurnal tidal amplitudes in zonal winds at 90 km over Tirunelveli is shown in Fig. 2e. It can be inferred that the semi-diurnal tidal amplitude, which remains below about 10 m/s during the rest of the period, increases to more than 15 m/s during day numbers 40–45 when ozone VMR maximizes (10 ppm) over equatorial latitudes. The tidal amplitude remains greater than 15 m/s up to day number 60, immediately after the maximum ozone VMR over equator at 36 km altitude. The ozone VMR decreases after the day number 60 to its pre-warming values (9 ppm) and the semi-diurnal tidal amplitude also decreases to less than 10 m/s. It can be noted that the diurnal tidal amplitudes show less values when semi-diurnal tidal amplitudes are larger during the SSW events. The correlation coefficient between ozone VMR at the equator and the semi-diurnal tidal amplitude is calculated to be 0.56 with lower and upper bounds for a 95% confidence interval of 0.39 and 0.68. At 10°N, it is 0.6 (0.45–0.72) and at 20°N, it is 0.55 (0.38–0.67).

Fig. 3a–f is same as Fig. 2a–f except that it is plotted for day numbers 1–90 days starting from 01 December 2008. Fig. 3a shows the state of high-latitude winter hemisphere using ERA-interim zonal mean temperature and zonal mean zonal winds. During the beginning of January 2009, normal winter conditions can be observed with poleward decrease in temperature inferred from the negative polar temperature gradient and prevailing eastward winds at polar latitudes. However, a major SSW event can be identified during January 21–27 from the positive polar temperature difference associated with the reversal of winds from eastward to westward at 10 hPa. According to Manney et al. (2009), the 2009 SSW event is remarkable, as it is characterized by a split polar vortex. The high-latitude stratopause altitude dropped dramatically and broke down, then reformed at very high (75–80 km) altitude. The ozone mixing ratio at 50°N around 95 km decreases from 10 ppm from day number 1 to around 6 ppm before the onset of the SSW event. It again increases to 8–9 ppm during day numbers 50–60, which includes the high-latitude warming event. After the end of the warming event, it increases to the pre-warming value of around 9 ppm around day number 70. The equatorial mesospheric ozone VMR does not show any clear variation in connection with the SSW events. Though there is a small decrease of VMR from 7 to 6 ppm for a short time of 50–55 coinciding with the warming event, there is not much variation at high-latitude stratospheric ozone VMR. However, the equatorial ozone increases from 10 to 11 ppm from day number 50 and it remains around 11 ppm during day numbers 60–75 and greater than 10 ppm until the end of the observation period shown in the figure. In this case as well, the latitudinal variation of temperature at 36 km shows the meridional temperature gradient reversing during the warming event with higher temperature (270 K) at high latitudes and lower temperature (230 K) at low latitudes. The ozone VMR at 36 km increases from 8.5 to 9 ppm from day number 30 and it increases further to 9.5 ppm during day numbers 50–60, when warming event occurred at high latitudes. The semi-diurnal tidal amplitude increases from 5–10 m/s around day number 50 to greater than 25 m/s on day number 60, when high ozone VMR is present over equator. After the day number 60, the semi-diurnal tidal amplitude decreases slightly and it remains greater than 15 m/s mostly until the end of the period shown in the figure. The correlation

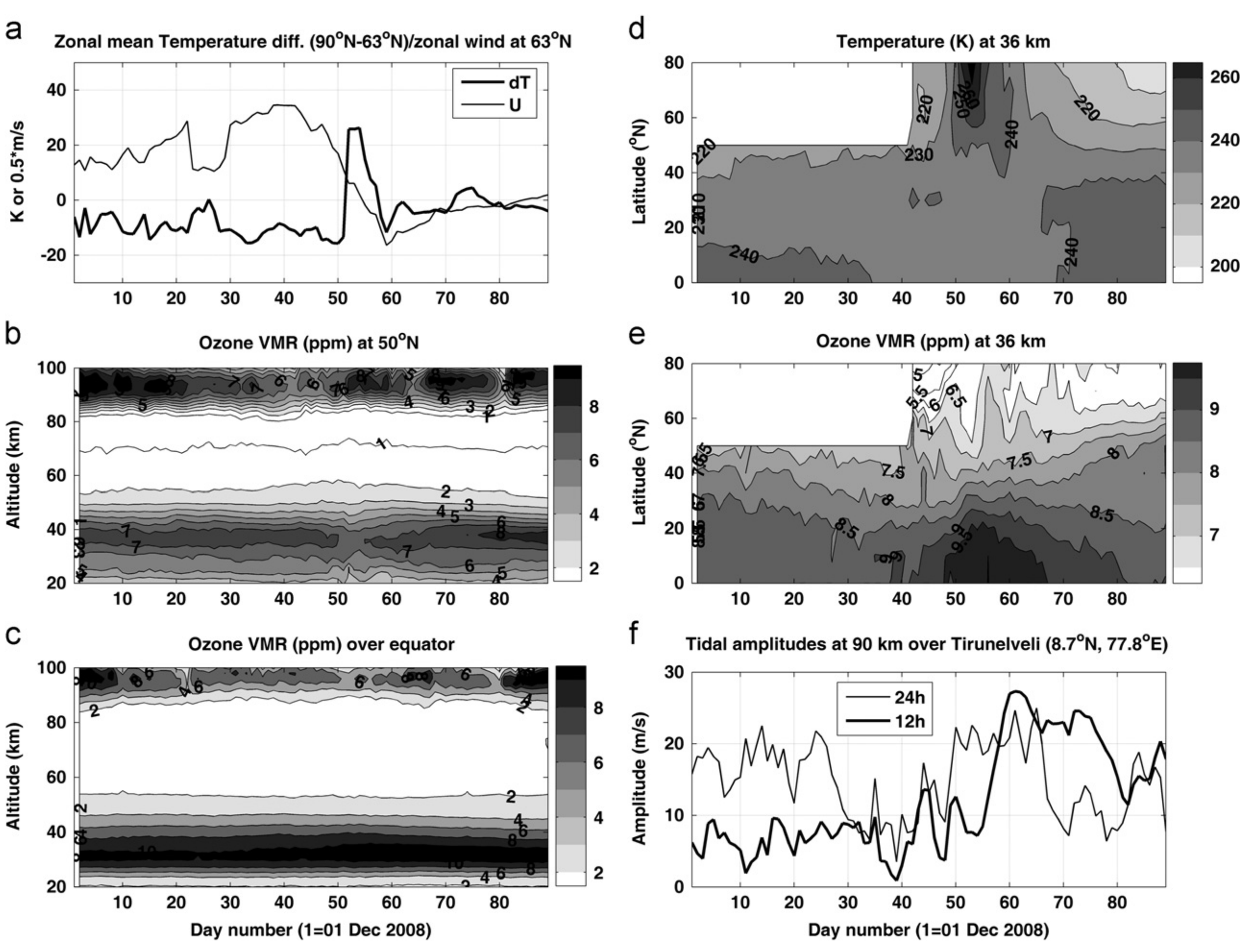

Fig. 3. Same as Fig. 2 except that it is plotted for day numbers 1–90 days starting from 01 December 2008.

coefficient between ozone VMR at the equator and the semi-diurnal tidal amplitude is calculated to be 0.7 (0.62–0.81). At 10°N and 20°N, it is 0.61 (0.46–0.73) and 0.58 (0.42–0.7), respectively. As noted earlier, the diurnal tidal amplitude shows less values, when semi-diurnal tidal amplitude is larger, in particular during the day numbers 65–80.

Though the enhancement of semi-diurnal tidal amplitude can be understood because of larger ozone VMR over equator, where solar insolation is more, the suppression diurnal tidal amplitude is unclear. As the diurnal tidal variabilities depend strongly on two mechanisms, namely, the non-linear interaction between tides and planetary waves and variations of source mechanism, we investigate which mechanism is more effective during the warming events. As Lieberman et al. (2003) suggested that tropospheric heating by water vapour absorption of near-infrared (IR) radiation is a leading drive of the propagating diurnal tide, the variation of ERA-interim specific humidity in the troposphere is examined.

Fig. 4 shows daily variation of zonal mean specific humidity over equator at 300, 500 and 700 hPa for 1–90 days starting from 01 December 2005 (left panels) and from 01 December 2008 (right panels). The daily variations of diurnal and semi-diurnal tidal amplitudes in zonal winds are plotted for comparison. There appears to be a relationship between specific humidity variations in particular at 300 hPa and diurnal tidal amplitude variations at 90 km in both the years (2005–06 and 2008–09). In the case of 2005–06, the extended larger values of specific humidity are noticed between day numbers 40–48. Similar extended large values of diurnal tidal amplitudes are observed at an earlier period during day numbers 35–44. An increasing trend is noticed in specific humidity value at 300 hPa after the day number 50. Remarkably, the diurnal tidal amplitude also shows an increasing trend after the day number 50 Minimum in specific humidity is observed around day numbers 30 and 50. Similarly diurnal tidal amplitudes also show smaller values during this time. The relation between specific humidity at 300 hPa and diurnal tidal amplitude at 90 km is more noteworthy in the case of 2008–09. The time variations of both go hand-in-hand with each other. The maximum values observed in specific humidity around day numbers 14, 25, 39, 51–67, 75 and 88. Similarly, maximum tidal amplitudes are also observed during these times. It is worthy to note that the extended maximum values observed both in diurnal tidal amplitudes and specific humidity values not only at 300 hPa, but also at 500 and 700 hPa during day numbers 50–70.

The correlation coefficient between daily variation of specific humidity values at 300, 500 and 700 hPa over equator and diurnal tidal amplitudes over Tirunelveli is shown in Fig. 5 for 2005–06 (top panels) and 2008–09 (bottom panel). The maximum correlation of 0.55 (0.45) is obtained at a lag of 8 days (9 days) for the specific humidity at 300 hPa (500 hPa) for the case of 2005–06.

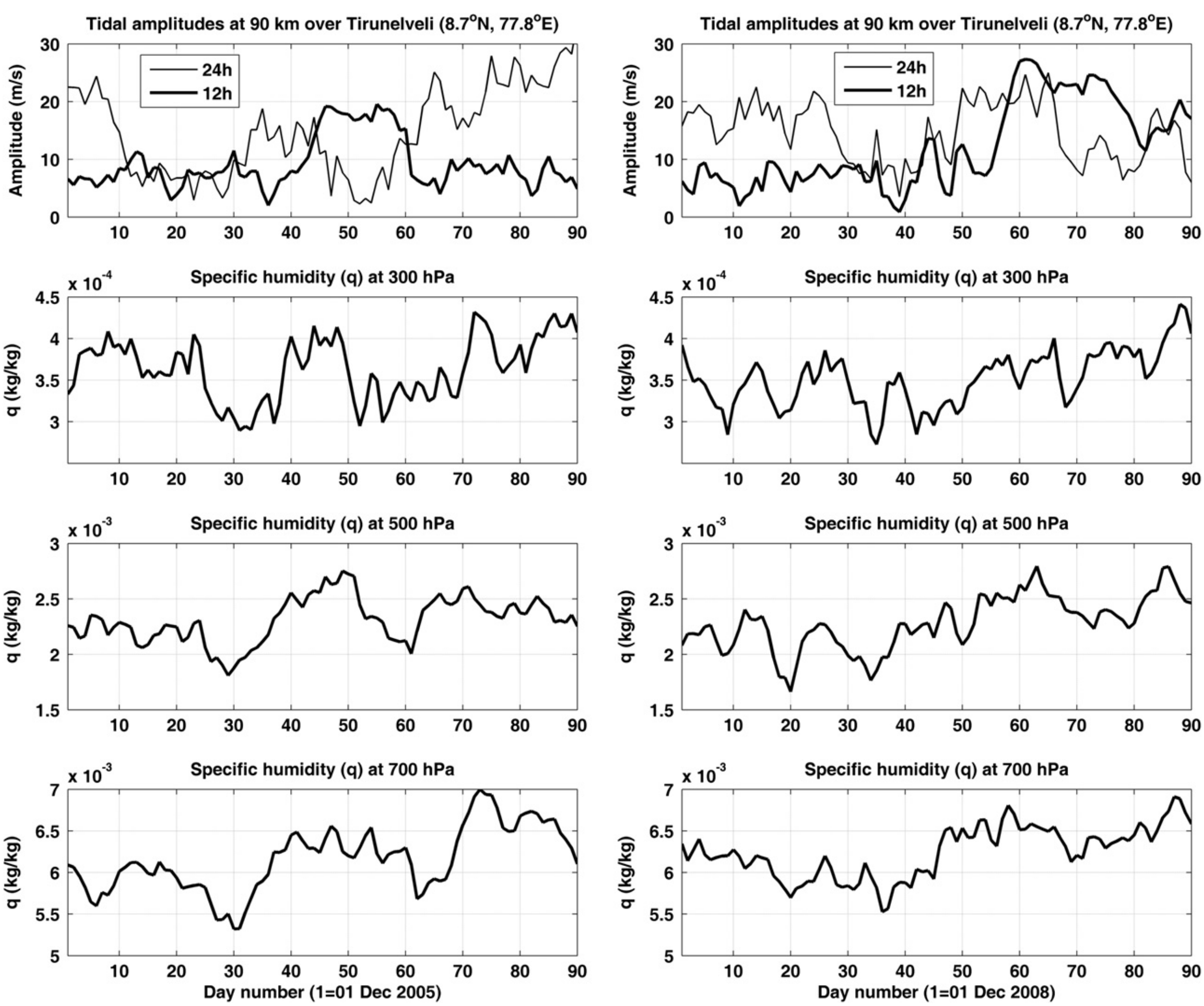

Fig. 4. Daily variation of zonal mean specific humidity over equator at 300, 500 and 700 hPa for 1–90 days starting from 01 December 2005 (left panels) and from 01 December 2008 (right panels). The daily variations of diurnal and semi-diurnal tidal amplitudes in zonal winds at 90 km are given in the top panels for comparison.

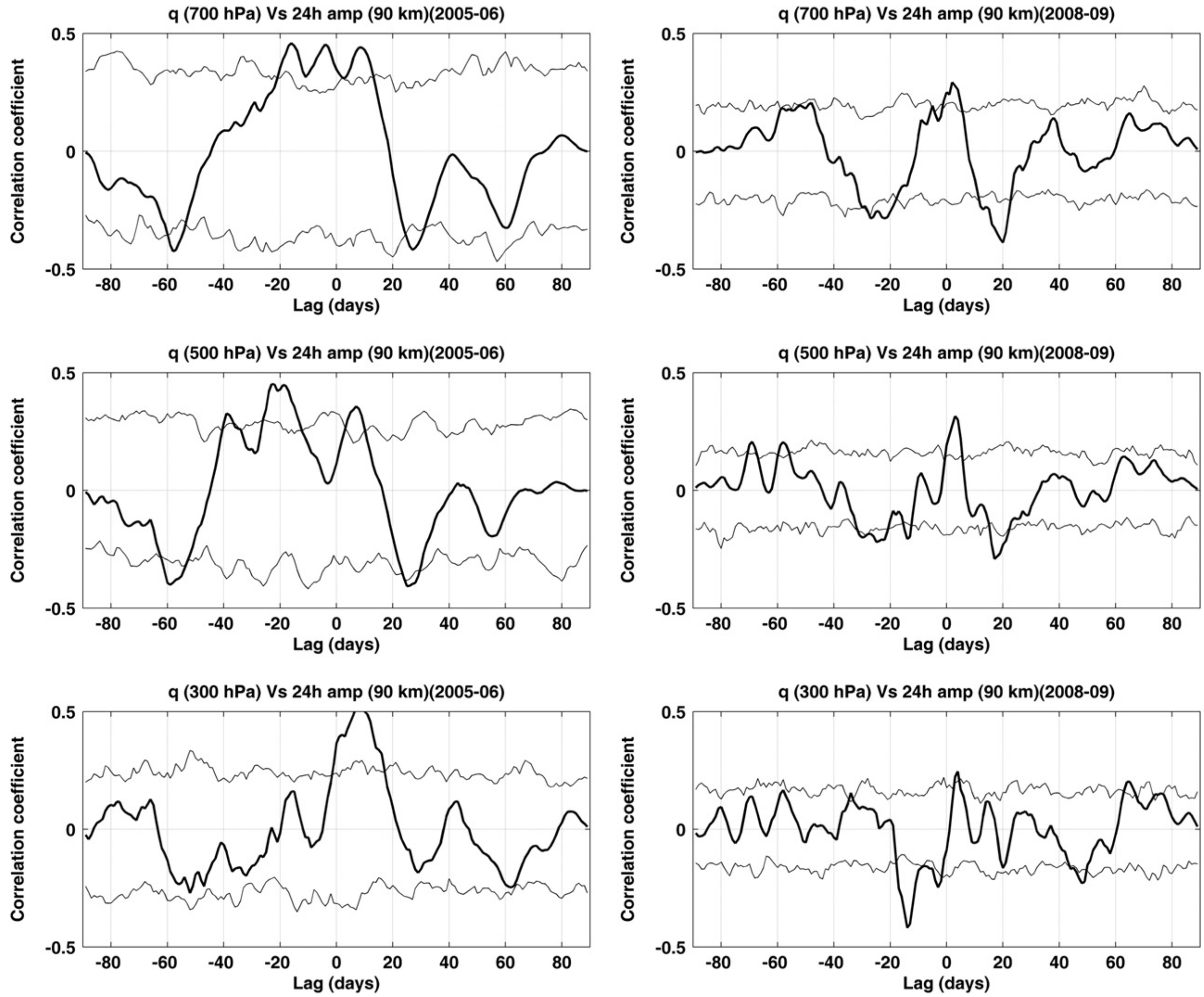

Fig. 5. Correlation coefficient between daily variation of zonal mean specific humidity values at 300, 500 and 700 hPa over equator and diurnal tidal amplitudes in zonal winds at 90 km for 2005–06 (left panels) and 2008–09 (right panels). 95% of all cross correlation coefficients would fail between the two wavy horizontal lines.

For the case of 2008–09, the maximum correlation of 0.25–0.3 is obtained at a lag of 3–4 days. It indicates that the diurnal tidal maximum leads the specific humidity variations at low-levels. The larger correlation of the mesospheric diurnal tide with specific humidity variations at 300 hPa is consistent with the larger diurnal heating rate (1, 1) due to water vapour obtained by Groves, (1982b) at around 9 km.

The similar variabilities observed in diurnal tide in zonal wind at 90 km and tropospheric humidity could be attributed due to modulation of both by extra-long period waves (> 15 days) and intraseasonal oscillations. The modulation by extra-long period waves could be due to their non-linear interaction with tides. In the equatorial troposphere, intraseasonal variability is one of the dominant features of atmospheric parameters and is commonly known as Madden–Julian oscillation (MJO). Eckermann et al. (1997) reported that the intraseasonal periods observed in the zonal winds, diurnal tide and gravity waves in zonal winds of the MLT region are similar to the MJO periods and suggested that the MJO cannot propagate directly into the MLT region because of their slow phase speed but modulate the intensity of the upward propagating gravity waves and diurnal tides and that these induce intraseasonal variations in the MLT zonal winds through wave-induced driving of the mean flow.

To study whether there is modulation of planetary waves (PW) on tides, the daily variation of PW with zonal wavenumbers (k) 1–3 at 63°N and at 10 hPa is compared with that of tidal variabilities (Fig. 6). It can be inferred from the figure that the enhancement of PW with $k=1$ is dominant just before the onset of the 2006 warming and the amplitude gets reduced with the onset of the warming event, whereas the 2009 event warming is preceded by PW with $k=2$. The planetary waves refract towards equator as they propagate at high-latitude stratosphere and we may expect that they may undergo non-linear interaction with the tides propagating vertically at low-latitude mesospheric altitudes. As planetary wave activity reduced dramatically during and several days after the warming events, the tidal variabilities after the onset of the SSW events cannot be expected to be due to their non-linear interaction with planetary waves. In particular, the enhancement of semi-diurnal tide after the warming can be due to source variabilities.

4. Discussion and conclusion

In the present paper, the ozone variabilities at high and low latitudes are reported during major warming events of 2006 and 2009. In both cases, the ozone VMR at high and low latitudes decreases above 85 km during the warming event and it recovers to pre-warming values after the end of the events. Smith et al. (2009) already reported lower ozone VMR around 85 km at high

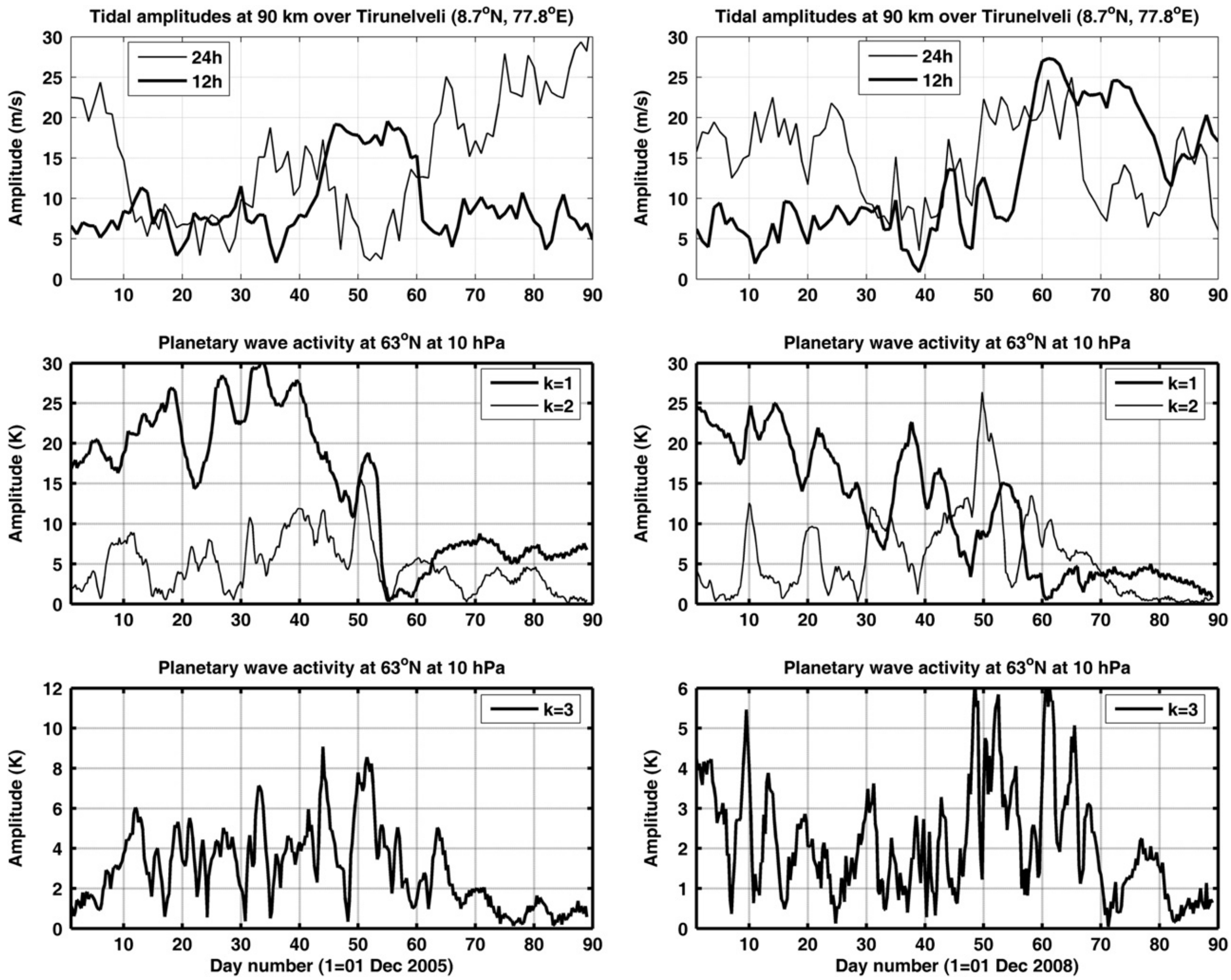

Fig. 6. Daily variation of planetary waves of zonal wavenumbers 1 and 2 (middle panels) and 3 (bottom panels) and daily variation of diurnal and semi-diurnal tidal amplitudes at 90 km over Tirunelveli (top panels) for a time interval of 1–90 days starting from 01 December 2005 (left panels) and 01 December 2008 (right panels).

latitudes during the SSW winters 2004, 2006 and 2009. The present study shows that even at low-latitude upper mesosphere, ozone mixing ratio is less when warming event occurs. At lower altitudes around 36 km, large VMR values are observed over equator and low latitudes, whereas lower VMR values are observed at high latitudes during the SSW events. In accordance with our observations, Randel (1993) earlier observed decrease in ozone at high latitudes and increase in ozone at low latitudes during warming events in the upper stratosphere. They observed reverse relationship in the lower stratosphere (50 hPa). As the forcing of the tides, in particular, semi-diurnal tide is mainly due to the absorption of ultraviolet radiation by ozone in the stratosphere and mesosphere, the tidal amplitudes at mesospheric heights were compared with the ozone variabilities at lower altitudes over equator. The large semi-diurnal tidal amplitude coincides with the reversed meridional temperature gradient with higher temperature at high latitude and lower temperature at low latitude. The increase of ozone at equator during the SSW events can be explained as follows. As meridional temperature gradient is reversed, the poleward circulation will reverse to equatorward circulation. The breakup of the polar vortex is characterized by large tongues of polar air stripped from the vortex and drawn to increasingly narrow filaments in middle and low latitudes (Manney et al., 1994b). As planetary wave activity has been observed to decrease with the onset of the warming event (Hoffmann et al., 2007; Sathishkumar and Sridharan, 2009), the Brewer Dobson circulation will become too weak to transport ozone to high latitudes from equator and low latitudes, where production is larger. As the transport to polar latitudes becomes weaker, the ozone produced at low latitudes remains at low latitudes till the meridional temperature gradient is reversed. The semi-diurnal tidal amplitudes, as expected, enhance, when ozone values are larger. The large semi-diurnal tidal amplitude coincides with the reversed meridional temperature gradient with higher temperature at high latitude and lower temperature at low latitude. Though the enhancement of semi-diurnal tidal amplitude can be understood, the reason for decrease of diurnal tidal amplitude during the SSW events is due mostly to the variations in the water vapour in the troposphere, in particular, at 300 hPa. Earlier, based on monthly diurnal water vapour IR heating rates derived using the National Centers for Environmental Prediction/National Center for Atmospheric Research (NCEP/NCAR) reanalysis and a global precipitable water data set, Lieberman et al. (2003) suggested that tropical tropospheric variability may be communicated to the diurnal tide (and possibly the middle and upper atmosphere) by means of water vapour heating. Though observations do show the linkage between SSW and low-latitude tidal variabilities, the non-linear interaction between tides and planetary waves producing non-migrating tides during the SSW events as noted by Pedatella and Forbes (2010) cannot be ruled out. Further, the relationship between the low-latitude tidal variabilities and the SSW events is yet to be firmly established based on more coordinated observations along with theoretical modeling works.

Acknowledgements

The authors acknowledge ECMWF for ERA-Interim data sets used in this study. They also acknowledge TIMED-SABER team for providing valuable data sets, in particular temperature and ozone used in this study, to make available to the word scientific community through the website http://saber.gats-inc.com/. The authors thank the two reviewers for their comments and suggestions, which helped them to improve their manuscript.

References

Bhattacharya, Y., Shepherd, G.G., Brown, S., 2004. Variability of atmospheric winds and waves in the Arctic polar mesosphere during a stratospheric sudden warming. Geophysical Research Letters 31, L23101. doi:10.1029/2004GL020389.

Briggs, B.H., 1984. The analysis of spaced sensor records by correlation techniques. Handbook for MAP 13, 166–186.

Eckermann, S.D., Rajopadhyaya, D.K., Vincent, R.A., 1997. Intraseasonal wind variability in the equatorial mesosphere and lower thermosphere: long-term observations from the central Pacific. Journal of Atmospheric Terrestrial Physics 59, 603–627. doi:10.1016/S1364-6826(96)00143-5.

Gurubaran, S., Rajaram, R., 2000. Signatures of equatorial electrojet in the mesospheric partial reflection drifts over magnetic equator. Geophysical Research Letters 27, 943–946.

Groves, G.V., 1982Ch. Hough components of ozone heating. Journal of Atmospheric and Terrestrial Physics 22, 111–121.

Groves, G.V., 1982b. Hough components of water vapor heating. Journal of Atmospheric and Terrestrial Physics 22, 281–290.

Hoffmann, P., Singer, W., Keuer, D., Hocking, W.K., Kunze, M.K., Murayama, Y., 2007. Latitudinal and longitudinal variability of mesospheric winds and temperature during stratospheric warming events. Journal of Atmospheric and Solar-Terrestrial Physics 69, 2355–2366.

Holton, J.R., 1976. A semi-spectral numerical model for wave-mean flow interactions in the stratosphere: applications to sudden stratospheric warmings. Journal of the Atmospheric Sciences 33, 1639–1649.

Jacobi, Ch., et al., 1999. Climatology of the semidiurnal tide at 52°N–56°N from ground-based radar wind measurements 1985–1995. Journal of Atmospheric and Solar-Terrestrial Physics 61, 975–991.

Lieberman, R.S., Ortland, D.A., Yarosh, E.S., 2003. Climatology and interannual variability of diurnal water vapour heating. Journal of Geophysical Research 108 ACL 8-1-8-18.

Matsuno, T., 1971. A dynamical model of the stratospheric sudden warming. Journal of the Atmospheric Sciences, 1479–1494.

Manney, G., Froidevaux, L., Waters, J.W., Zurek, R.W., Read, W.G., Elson, L.S., Kumer, J.B., Mergenthaler, J.L., Roche, A.E., 'Neill, A.O., Harwood, R.S., Mackenzie, I., Swinbank, R., 1994a. Chemical depletion of ozone in the Arctic lower stratosphere during winter 1992–93. Nature 370, 429–434.

Manney, G.L., Zurek, R.W., O'Neill, A., Swinbank, R., 1994b. On the motion of air through the stratospheric polar vortex. Journal of the Atmospheric Sciences 51, 2973–2994.

Manney, G.L., et al., 2008. The evolution of the stratopause during the 2006 major warming: satellite data and assimilated meteorological analyses. Journal of Geophysical Research 113, D11115. doi:10.1029/2007JD009097.

Manney, G.L., Schwartz, M.J., Krüger, K., Santee, M.L., Pawson, S., Lee, J.N., Daffer, W.H., Fuller, R.A., Livesey, N.J., 2009. Aura Microwave Limb Sounder observations of dynamics and transport during the record-breaking 2009 Arctic stratospheric major warming. Geophysical Research Letters 36, L12815. doi:10.1029/2009GL038586.

McIntyre, M.E., 1982. How well do we understand the dynamics of stratospheric warmings? Journal of Meterological Society of Japan 60, 37–65.

Pedatella, N.M., Forbes, J.M., 2010. Evidence of stratospheric sudden warming-ionosphere coupling due to vertically propagating tides. Geophysical Research Letters 37, L11104. doi:10.1029/2010GL043560.

Rajaram, R., Gurubaran, S., 1998. Seasonal variabilities of low latitude mesospheric winds. Annales Geophysicae 16, 197–204.

Randel, W.J., 1993. Global variations of zonal mean ozone during stratospheric warming events. Journal of the Atmospheric Sciences 50 (3308–3321), 1993.

Remsberg, E.E., et al., 2008. Assessment of the quality of the retrieved temperature versus pressure profiles in the middle atmosphere from TIMED/SABER. Journal Geophysical Research 113, D17101. doi:10.1029/2008JD010013.

Rogers, A.E.E., Lekberg, M., Pratap, P., 2009. Seasonal and diurnal variations of ozone near the mesopause from observations of the 11.072-GHz Line. Journal of Atmospheric and Oceanic Technology 26, 2192–2199.

Sathishkumar, S., Sridharan, S., 2009. Planetary and gravity waves in the mesosphere and lower thermosphere region over Tirunelveli (8.7°N, 77.8°E) during stratospheric warming events. Geophysical Research Letters 36, L07806. doi:10.1029/2008GL037081.

Smith, A.K., López-Puertas, M., Garcia-Comas, M., Tukiainen, S., 2009. Saber observations of mesospheric ozone during NH later winter 2002–2009. Geophysical Research Letters 36, L23804. doi:10.1029/2009GL040942.

Sridharan, S., Sathishkumar, S., Gurubaran, S., 2009. Variabilities of mesospheric tides and equatorial electrojet strength during major stratospheric warming events. Annales Geophysicae 27, 4125–4130.